Brief Article

Boosting anti-inflammatory potency of zafirlukast by designed polypharmacology

Simone Schierle, Cathrin Flauaus, Pascal Heitel, Sabine Willems, Jurema Schmidt, Astrid Kaiser, Lilia Weizel, Tamara Goebel, Astrid Kahnt, Gerd Geisslinger, Dieter Steinhilber, Mario Wurglics, G. Enrico Rovati, Achim Schmidtko, Ewgenij Proschak, and Daniel Merk

Just Accepted

Boosting anti-inflammatory potency of zafirlukast by designed polypharmacology

Simone Schierle[a]#, Cathrin Flauaus[b]#, Pascal Heitel[a], Sabine Willems[a], Jurema Schmidt[a], Astrid Kaiser[a], Lilia Weizel[a], Tamara Goebel[a], Astrid Kahnt[a], Gerd Geisslinger[c], Dieter Steinhilber[a], Mario Wurglics[a], G. Enrico Rovati[d], Achim Schmidtko[b], Ewgenij Proschak[a]##, Daniel Merk*[a]##

[a] Institute of Pharmaceutical Chemistry, Goethe University Frankfurt, Max-von-Laue-Str. 9, D-60438 Frankfurt, Germany

[b] Institute of Pharmacology, College of Pharmacy, Goethe University Frankfurt, Max-von-Laue-Str. 9, D-60438 Frankfurt, Germany

[c] Institute of Clinical Pharmacology, Goethe University Frankfurt, Theodor-Stern-Kai 7, D-60590 Frankfurt, Germany

[d] Institute of Pharmacological Sciences, University of Milan, Via Balzaretti 9, I-20133 Milan, Italy

* E-mail: merk@pharmchem.uni-frankfurt.de

KEYWORDS: multi-target design • drug repurposing • selective optimization of side-activities • inflammation

ABSTRACT: Multi-target design offers access to bioactive small molecules with potentially superior efficacy and safety. Particularly multifactorial chronic inflammatory diseases demand multiple pharmacological interventions for stable treatment. By minor structural changes, we have developed a close analogue of the cysteinyl-leukotriene receptor antagonist zafirlukast that simultaneously inhibits soluble epoxide hydrolase and activates peroxisome proliferator-activated receptor γ. The triple modulator exhibits robust anti-inflammatory activity in vivo and highlights the therapeutic potential of designed multi-target agents.

INTRODUCTION

Though anti-inflammatory drug discovery is very intensive[1], inflammatory diseases remain amongst the most serious health burdens and there is unmet medical need for more efficacious anti-inflammatory drugs. The number of drugged targets in inflammatory diseases is constantly growing but especially in the most severe, chronic disorders even innovative agents fail to produce sufficient therapeutic efficacy[1]. As a very complex pathophysiological process, inflammation involves a myriad of enzymes, mediators and receptors and pharmacological modulation of a single target tends to cause shunting effects that compromise therapeutic efficacy[2]. Thus, robust anti-inflammatory therapies often require the use of multiple drugs but considering the drawbacks of excessive polypharmacy, a multi-target anti-inflammatory agent seems a superior approach.

RESULTS & DISCUSSION

To generate such multi-target anti-inflammatory agent, we selected the cysteinyl leukotriene receptor 1 (CysLT₁R)[3,4] antagonist zafirlukast (**1**)[5] for which we have
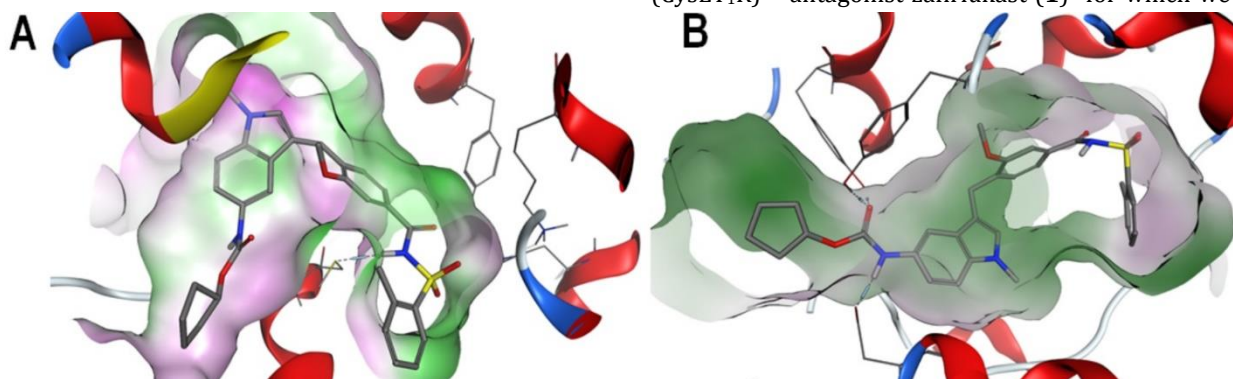
Figure 1. Docking analysis of the lead compound's (**1**) binding mode in the PPARγ ligand binding domain (A, PDB-ID: 3WMH) and the sEH active site (B, PDB-ID: 5ALZ). Detailed views of the individual molecular building blocks and docking-derived structural modifications are shown in Figures S1&S2.
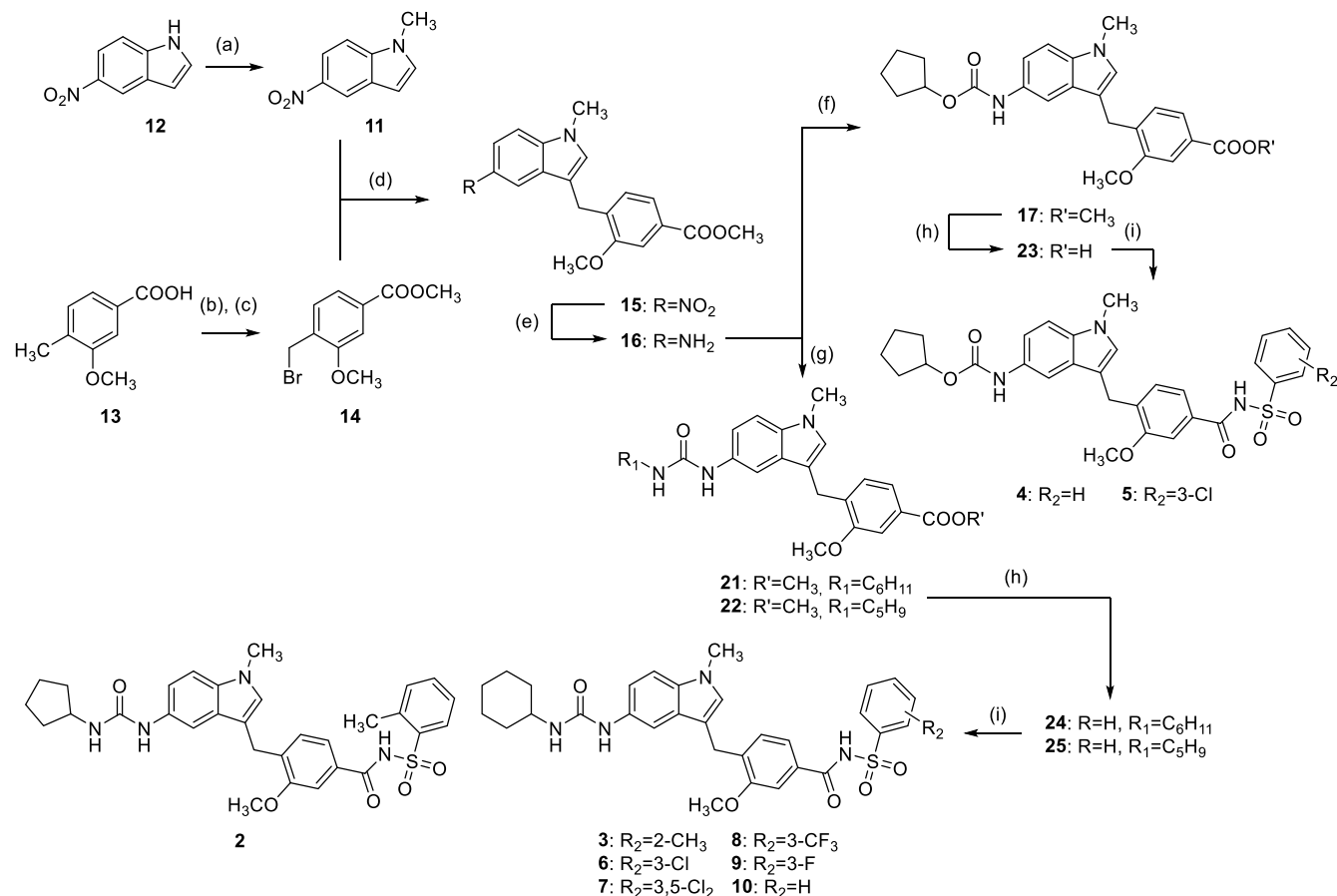
Scheme 1. Synthesis of **2**-**10**. Reagents & conditions: (a) Me$_2$SO$_4$, dioxane, 40 °C, 2.5 h; (b) MeOH, SOCl$_2$, reflux, 4 h; (c) CHCl$_3$, AIBN, NBS, reflux, 4 h; (d) FeCl$_3$, dioxane, r.t. 12 h; (e) H$_2$, Pd(C), MeOH, r.t. 12 h; (f) THF, DIPEA, C$_5$H$_9$-OCOCl (**18**), 4 °C -> r.t., 4 h; (g) THF, DBU, C$_6$H$_{11}$-NCO (**19**) or C$_5$H$_9$-NCO (**20**), 40 °C, 12 h; (h) LiOH, MeOH/H$_2$O, r.t., 16 h; (i) CHCl$_3$, DCC, DMAP, R$_2$-Ph-SO$_2$NH$_2$ (**26-30**), reflux, 12 h.

observed moderate off-target activity (Table 1) on the peroxisome proliferator-activated receptor γ (PPARγ)[6] and the soluble epoxide hydrolase (sEH)[7]. Like CysLT$_1$R, PPARγ and sEH interact with metabolites of arachidonic acid and hold great anti-inflammatory potential[1] and their selective modulation reduced acute inflammation in animal models[8,9]. The weak side-activities of the fatty acid mimetic[10] **1**, therefore, seem supportive of an anti-inflammatory efficacy and we aimed to optimize the PPARγ agonistic and sEH inhibitory activity of **1** while retaining CysLT$_1$R antagonism to generate a triple modulator that simultaneously addresses three anti-inflammatory targets.

To establish a strategy for structural optimization, we analyzed the putative binding mode of **1** in the PPARγ ligand binding domain (PDB-ID: 3WMH) and the sEH C-terminal domain (PDB-ID: 5ALZ[11]) by molecular docking (Figure 1, detailed view in Figures S1&S2). Examination of the best scored poses suggested that minor changes would allow marked improvements in potency. Spatial extension of the urethane cyclopentyl substituent to a six-membered ring seemed favorable for PPARγ and sEH binding since the urethane *O*-substituent protruded into lipophilic sub-pockets of both targets which offered additional space for a larger ring. Moreover, caused by its *ortho*-methyl residue, the phenylsulfonamide obtained a dihedral conformation that was disfavored by PPARγ and might be resolved through a

free *ortho*-position which was supported by strain energy calculations (Table S1). Interaction potential analysis in the phenylsulfonamide binding region in the PPARγ ligand binding site, furthermore, suggested opportunities for optimization in *meta*- or *para*-substitution of said ring with small halogens. And finally, replacement of the urethane moiety in **1** by urea appeared to optimize sEH inhibitory potency by adding a further H-bond donor that would enable an additional H-bond towards Asp335. Guided by these *in silico* observations, we prepared analogues of **1** with small but concerted structural changes to enhance triple potency.
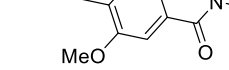
Analogues **2**-**10** were prepared in an eight-step synthetic procedure adopted from a published[12] approach to **1** with suitable modifications (Scheme 1). In brief, *N*-methyl-5-nitroindole (**11**) was available from **12** by methylation with DMS. Esterification of **13** followed by radical bromination yielded building block **14** which was coupled with **11** to **15** under Friedel-Craft conditions using FeCl$_3$ as catalyst. After reducing **15** with H$_2$ and Pd(C) to aniline **16**, urethane **17** was available from **16** and chloroformate **18** while reaction of **16** with isocyanates **19** and **20** produced ureas **21** and **22**. Finally, ester hydrolysis in **17**, **21** and **22** to free acids **23-25** followed by sulfonamide coupling with DCC/DMAP and **26-30** afforded **2-10** in 8-12% overall yield.

PPARγ agonistic potency of analogues **2**-**10** was quantified in a specific reporter gene assay[13] in HEK293T cells

based on a hybrid receptor comprising the PPARγ-LBD and the DNA-binding domain of the nuclear receptor Gal4 from yeast. Inhibition of sEH was determined in a fluorescence-based assay[14] with recombinant protein and PHOME as fluorogenic substrate. A cellular leukotriene D_4 induced Ca^{2+}-influx assay in Cos-7 cells transiently overexpressing $CysLT_1R$[15] served to characterize antagonistic potency of **2-10** on $CysLT_1R$ (Table 1).

Based on our docking study, we replaced the urethane moiety of **1** by a urea (**2**) which expectedly was accompanied by a significant improvement in sEH inhibitory potency while $CysLT_1R$ antagonism dropped dramatically. On PPARγ, replacement of the urethane moiety by urea hardly affected the EC_{50} value but significantly diminished transactivation efficacy. Considering that weight gain is a common adverse effect of full PPARγ agonists and that partial agonists lack this undesired activity while retaining anti-inflammatory effects of PPARγ modulation[16–18], partial agonistic activity on PPARγ appears favorable and safer.

Ring expansion from cyclopentylurea **2** to cyclohexylurea **3** further promoted sEH inhibition and markedly improved PPARγ agonism but was poorly tolerated concerning $CysLT_1R$ antagonism. Variations in the sulfonamide moiety were better tolerated by $CysLT_1R$ with unsubstituted phenylsulfonamide **4** and 3-chlorophenylsulfonamide **5** retaining a pA_2 value above 10. As suggested by the proposed binding mode, the freely rotatable phenylsulfonamides **4** and **5** strongly enhanced PPARγ agonistic potency. Inhibitory potency on sEH was hardly affected by changes in the sulfonamide region. Thus, we combined cyclohexylurea (**3**) and 3-chlorophenylsulfonamide (**5**) as most favorable modifications for sEH inhibition and PPARγ agonistic potency, respectively. The resulting compound **6** comprised balanced triple modulatory potency on PPARγ, sEH and $CysLT_1R$. Introduction of a second chlorine atom in **7** and replacement of chlorine by trifluoromethyl (**8**) failed to improve the triple activity while replacement of chlorine by fluorine (**9**) was slightly favored by PPARγ and sEH but not by CysLT1. Intriguingly, the most favorable triple activity profile was achieved with unsubstituted phenylsulfonamide **10**. As assumed from the proposed binding poses, three minor structural changes were sufficient to generate

a triple modulator with nanomolar potency on PPARγ, sEH and $CysLT_1R$.

Off-target profiling of **1** and **10** on nuclear receptors (Figure S3A) revealed significantly reduced off-target activity for the triple modulator **10** despite its designed polypharmacological profile while **1** turned out remarkably unselective. Especially its agonistic activity on pregnane X receptor (PXR) and constitutive androstane receptor (CAR) may compromise the safety of **1** since these xenobiotic receptors drive cytochrome P450 expression, promote drug metabolism and can be a basis of drug-drug interactions[19,20]. In contrast to **1**, the triple modulator **10** was inactive on CAR and only weakly activated PXR.

Moreover, the triple modulator **10** comprised remarkably higher aqueous solubility (**10**: 2.1 mg/L; **1**: 0.14 mg/L) and a lower $logD_{7.4}$ value (**10**: 1.70; **1**: 2.47) than **1**, and was considerably less toxic (Figure S3B-D). Microsomal stability was high for both, **10** and lead structure **1** with 65% and 73%, respectively, remaining after 4 hours incubation (Figure S1E). Under cellular conditions, **10** robustly inhibited sEH product formation in HepG2 homogenates with an IC_{50} value of 14±2 nM and induced PPARγ target gene expression in HepG2 cells (Figure 2A/B). However, in contrast to PPARγ agonist rosiglitazone, **10** did not induce adipocyte differentiation and failed to induce PPARγ regulated gene expression in this cell-type (Figure 2C/D). Thus, **10** comprises a non-adipogenic, selective PPARγ modulatory profile as it has been observed for other PPARγ ligands[18].

Pilot *in vivo* evaluation of **10** in four wild-type male C57Bl6/J mice (Figure 3A-C) revealed a favorable pharmacokinetic profile after oral application of 10 mg/kg **10** with rapid uptake, good bioavailability and a terminal half-life of 1.9 h resulting in effective concentrations for PPARγ activation over approx. 4 h. Sufficient concentrations of **10** for sEH inhibition and $CysLT_1R$ antagonism were still detectable after 8 h. The EET/DHET ratio was significantly shifted towards sEH substrates 8 h post dose and of expression PPARγ target gene CD36 was upregulated in mouse livers compared to vehicle treated animals.

Table 1. *In vitro* activity of **1-10** on PPARγ, sEH and $CysLT_1R$. Results are mean±SEM, $n≥3$.

ID	R_1	X	R_2	PPARγ EC_{50} [μM] (max. rel. act. [%])	sEH IC_{50} [μM]	$CysLT_1R$ (pA_2)
1	C_5H_9	O	2-CH_3	2.44±0.09 (129±4)	2.0±0.3	11.4±0.1
2	C_5H_9	NH	2-CH_3	2.49±0.09 (21±1)	0.59± 0.06	9.1±0.1
3	C_6H_{11}	NH	2-CH_3	0.67±0.05 (47±1)	0.15±0.01	7.6±0.1
4	C_5H_9	O	H	0.23±0.05 (140±8)	2.5±0.8	10.1±0.1
5	C_5H_9	O	3-Cl	0.14±0.01 (73±1)	7±2	10.0±0.1
6	C_6H_{11}	NH	3-Cl	0.37±0.03 (18±1)	0.68±0.06	8.9±0.1
7	C_6H_{11}	NH	3,5-Cl_2	0.74±0.03 (29±1)	0.55±0.01	8.2±0.2
8	C_6H_{11}	NH	3-CF_3	0.35±0.05 (18±1)	1.49±0.09	8.3±0.1
9	C_6H_{11}	NH	3-F	0.20±0.02 (21±1)	0.41±0.02	7.9±0.1
10	C_6H_{11}	NH	H	**0.30±0.02 (36±1)**	**0.043±0.002**	**8.7±0.1**
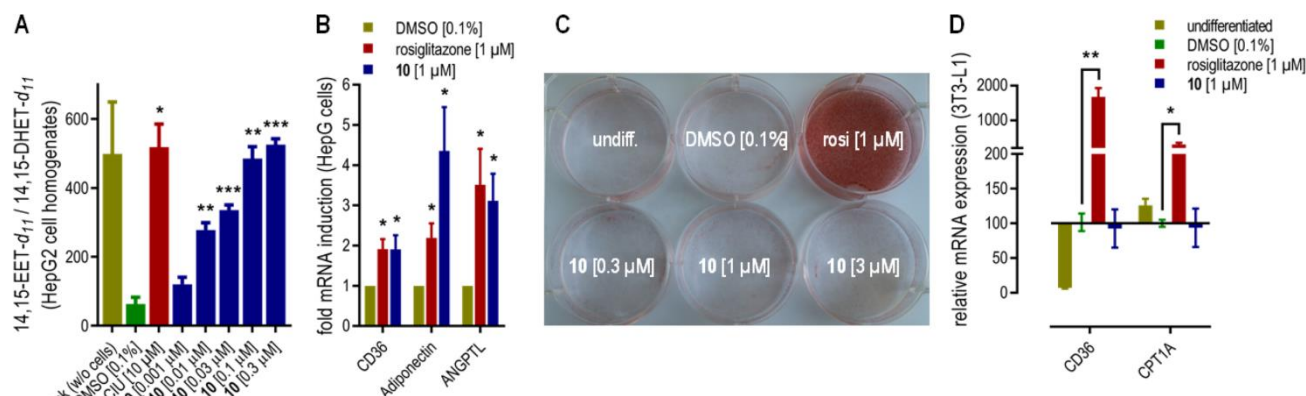
Figure 2. *In vitro* pharmacological characterization of triple modulator **10**: (A) **10** inhibits sEH product formation with an IC_{50} value of 14±2 nM in HepG2 cells. (B) Moreover, **10** induces PPARγ target gene transcription in HepG2 cells. (C/D) However, **10** does not promote adipocyte differentiation (C) or PPARγ target gene transcription in 3T3-L1 mouse fibroblasts (D). Results are mean±SEM, n=4, * $p < 0.05$, ** $p < 0.01$, $p < 0.001$. CIU - *N*-cyclohexyl-*N'*-(4-iodophenyl)urea.

Encouraged by the favorable *in vitro* and pilot *in vivo* data, we studied anti-inflammatory activity of **10** in the model of paw edema induced by intraplantar injection of zymosan in mice, which closely mimics the symptoms of inflammation in man[21] (Figure 3D). **1** (10 mg/kg), **10** (10 mg/kg) or vehicle were administered orally 30 min prior to zymosan, and the paw edema was assessed by plethysmometry. 8 h after zymosan injection, the paw edema was indistinguishable between groups. 24 h after zymosan injection, the paw edema was significantly reduced in mice treated with **10** compared to vehicle-treated mice whereas **1** did not affect the extent of paw edema. Control experiments revealed no change in paw size in the contralateral hindpaw. These data confirm that **10** exerts anti-inflammatory effects *in vivo* and that triple target modulation of **10** is superior to **1**.

PPARγ activation[9], e.g. with the full agonist rosiglitazone, as well as sEH inhibition[8] have revealed some therapeutic efficacy in animal models of acute inflammation similar to the paw edema model used in our study. Designing PPARγ agonistic and sEH inhibitory activity into **1** provided the triple modulator **10** with significantly superior anti-inflammatory effects compared to **1** in a murine model of acute inflammation. Notably, **10** only exhibits partial PPARγ agonism which proved sufficient to achieve this anti-inflammatory activity underlining a great advantage of multi-target modulation. When supportive target combinations are addressed simultaneously, partial modulation of these targets can be sufficient to achieve the desired therapeutic effects which may allow the development of multi-target compounds with high efficacy and reduced adverse activity[2].

The triple modulatory potency of **10** may be of therapeutic value in a variety of diseases involving inflammatory processes. Particularly, in allergic asthma for which **1** is approved, PPARγ plays a central role in the regulation of airway inflammation involving modulation of IL-17 production[22] and eosinophil differentiation[23]. Accordingly, PPARγ agonists showed therapeutic efficacy in animal models of allergic asthma including anti-inflammatory and bronchodilatory activity[22,24,25]. Even a correlation of PPARγ polymorphisms with asthma development has been reported[26]. Moreover, sEH inhibition reduced allergic airway inflammation and hyperresponsiveness in ovalbumin induced asthma in mice[27] suggesting that all three molecular targets of **10** are suitable to treat allergic asthma.

Beyond asthma, chronic obstructive pulmonary disease (COPD) may also markedly profit from PPARγ activation combined with inhibition of $CysLT_1R$ and sEH. Recent clinical observations have found decreased expression of PPARγ in lung tissue of COPD patients[28] and reduced COPD exacer-
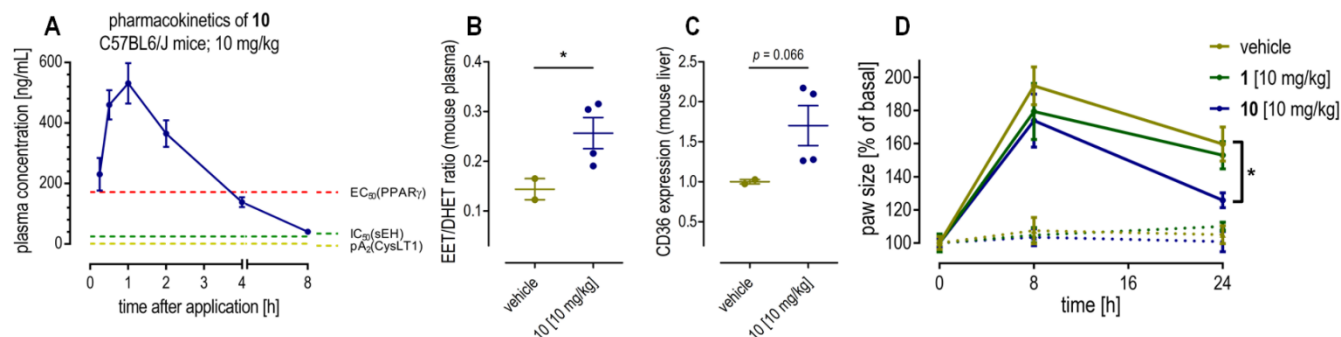
Figure 3. *In vivo* pharmacological characterization of triple modulator **10**: Pharmacokinetic profiling of **10** after a 10 mg/kg p.o. dose revealed rapid uptake, high bioavailability and a half-life of 2 h (A, results are mean±SEM; n=4). In healthy male wild-type C57BL6/J mice, **10** increased plasma sEH substrate/product ratio (B) and modulated hepatic transcription of PPARγ target gene CD36 (C, results are mean±SEM; n(vehicle)=2, n(**10**)=4). In the paw edema model in C57BL/6N mice pretreated with vehicle, **1** or **10** 30 min prior to zymosan injection into one hindpaw (D), **10** significantly reduced paw edema after 24 h suggesting anti-inflammatory potency in vivo and was superior to lead compound **1** confirming increased efficacy through designed multi-target activity (solid lines - ipsilateral paw; dotted lines - contralateral paw; results are mean±SEM; n=6). * $p < 0.05$.

bations in patients receiving PPARγ agonistic thiazolidinediones[29]. Moreover, treatment with CysLT1R antagonist **1** improved the lung function of COPD patients[30] and sEH inhibitors possessed therapeutic efficacy in COPD mouse models[31,32]. The rational combination of simultaneously modulating these three biological targets with a single molecule may, therefore, produce superior therapeutic efficacy in COPD.

CONCLUSION

The development of triple modulator **10** and its activity profile compared to **1** highlight the remarkable impact of very minor structural changes on a drug's effects and efficacy. Concerted optimization of intrinsic off-target activities of **1** generated the potent triple modulator **10** which by modulating three individual anti-inflammatory targets comprises significantly enhanced anti-inflammatory potency *in vivo* while conserving the lead compound's structural properties, molecular weight and pharmacokinetic profile. This alternative interpretation of selective optimization of side-activities[33] might hold great potential for numerous drug molecules, especially in times of increasing polypharmacy.

EXPERIMENTAL

General. All final compounds (**2**-**10**) for biological evaluation had a purity of >95% according to HPLC-UV analysis at wavelengths 245 and 280 nm.

Preparation and analytical characterization of triple modulator **10** and intermediates:

4-((5-(3-Cyclohexylureido)-1-methyl-1*H*-indol-3-yl)methyl)-3-methoxy-*N*-(phenylsulfonyl)benzamide (**10**): 4-((5-(3-Cyclohexylureido)-1-methyl-1*H*-indol-3-yl)methyl)-3-methoxybenzoic acid (**24**, 50 mg, 0.11 mmol, 1.00 eq) was dissolved in chloroform (abs., 10 mL) and benzenesulfonamide (**26**, 23 mg, 0.15 mmol, 1.30 eq), dicyclohexyl carbodiimide (35 mg, 0.17 mmol, 1.50 eq) and 4-(*N*,*N*-dimethylamino)pyridine (14 mg, 0.11 mmol, 1.00 eq) were added and the mixture was stirred under reflux for 12 h. After cooling to room temperature, 10 mL 5% aqueous hydrochloric acid were added, phases were separated, and the aqueous layer was extracted with EtOAc (3x10 mL). The combined organic layers were dried over Na_2SO_4 and the solvents were evaporated under reduced pressure. The crude product was purified by column chromatography using EtOAc/hexane/acetic acid (9:89:2) as mobile phase. The residue was then dissolved in 0.5 mL methanol, 10 mL water were added, and the suspension was immediately frozen and lyophilized to yield the title compound as colorless solid (50 mg, 76%). ^{1}H NMR (400 MHz, CDCl₃) δ = 8.15 (dd, *J* = 1.6, 1.6 Hz, 1H), 8.12 (dd, *J* = 1.7, 1.7 Hz, 1H), 7.67 – 7.58 (m, 1H), 7.53 (dd, *J* = 7.7, 7.7 Hz, 2H), 7.34 (d, *J* = 1.6 Hz, 2H), 7.27 (d, *J* = 1.9 Hz, 1H), 7.25 – 7.21 (m, 2H), 7.07 (d, *J* = 7.9 Hz, 1H), 7.01 (dd, *J* = 8.6, 1.9 Hz, 1H), 6.85 (s, 1H), 4.65 (d, *J* = 7.1 Hz, 1H), 4.03 (s, 2H), 3.87 (s, 3H), 3.74 (s, 3H), 1.85 – 1.77 (m, 2H), 1.62 – 1.46 (m, 3H), 1.34 – 1.20 (m, 5H). ^{13}C NMR (126 MHz, DMSO-*d₆*) δ = 165.12, 156.69, 154.98, 139.58, 135.39, 133.67, 132.82, 132.41, 129.32, 129.16, 128.33, 127.70, 127.40, 120.75, 114.28, 110.61, 110.05, 109.55, 107.52, 55.71, 47.59, 33.16, 32.32, 29.63, 25.31, 24.74, 24.45. MS (ESI-): *m/z* 573.24 [M-H]⁻. HRMS (MALDI): *m/z* calculated for $C_{31}H_{34}N_4O_5SNa$ 597.21421, found 597.21292 [M+Na]⁺.

1-Methyl-5-nitro-1*H*-indole (**11**): 5-Nitro-1*H*-indole (**12**, 2.45 g, 15.1 mmol, 1.0 eq) was dissolved in 100 mL DMF, NaOH (1.28 g, 32.0 mmol, 2.1 eq) was added and the mixture was stirred for 10 min at 40 °C. Dimethyl sulfate (1.68 mL, 17.7 mmol, 1.2 eq) was carefully added and the mixture was stirred for another 2 h at 40 °C. Then, H₂O was added to precipitate the title compound as a yellow solid (6.12 g, 23%). ^{1}H NMR (250 MHz, DMSO-*d₆*) δ = 8.55 (d, *J* = 2.2 Hz, 1H), 8.02 (dd, *J* = 9.1, 2.3 Hz, 1H), 7.62 (d, *J* = 9.1 Hz, 1H), 7.58 (d, *J* = 3.2 Hz, 1H), 6.73 (dd, *J* = 3.2, 0.6 Hz, 1H), 3.86 (s, 3H). MS (ESI+): no molecular ion.

Methyl 3-methoxy-4-methylbenzoate (**14a**): 3-Methoxy-4-methylbenzoic acid (**13**, 5.00 g, 30.1 mmol, 1.0 eq) was dissolved in MeOH (abs., 150 mL). Thionyl chloride (3.30 mL, 45.5 mmol, 1.5 eq) was carefully added, and the mixture was refluxed for 6 h. 50 mL 2 N aqueous hydrochloric acid were then added, and the mixture was extracted with CHCl₃ (3x50 mL). The combined organic layers were dried over MgSO₄ and the solvent was evaporated in vacuum to obtain the title compound as a colorless solid (4.26 g, 79%). ^{1}H NMR (250 MHz, DMSO-*d₆*) δ = 7.47 (d, *J* = 7.7 Hz, 1H), 7.42 (s, 1H), 7.27 (d, *J* = 7.7 Hz, 1H), 3.84 (s, 6H), 2.20 (s, 3H). MS (ESI+): no molecular ion.

Methyl 4-(bromomethyl)-3-methoxybenzoate (**14**): Methyl 3-methoxy-4-methylbenzoate (**14a**, 4.26 g, 23.7 mmol, 1.0 eq) was dissolved in 150 mL CHCl₃. *N*-Bromosuccinimide (5.12 g, 28.8 mmol, 1.2 eq) and azobisisobutyronitrile (377 mg, 2.3 mol, 0.1 eq) were added and the mixture was refluxed for 12 h. After cooling to room temperature, the precipitated title compound was filtered off as a colorless solid (3.81 g, 73%). ^{1}H NMR (250 MHz, DMSO-*d₆*) δ = 7.56 – 7.49 (m, 3H), 4.66 (s, 2H), 3.92 (s, 3H), 3.86 (s, 3H). MS (ESI+): no molecular ion.

Methyl 3-methoxy-4-((1-methyl-5-nitro-1*H*-indol-3-yl)methyl)benzoate (**15**): 1-Methyl-5-nitro-1*H*-indole (**11**, 699 mg, 4.00 mmol, 1.0 eq) and methyl 4-(bromomethyl)-3-methoxybenzoate (**14**, 1.00 g, 4.00 mmol, 1.0 eq) were dissolved in 1,4-dioxane (abs., 50 mL), FeCl₃ (1.94 g, 12.0 mmol, 3.0 eq) was carefully added, and the mixture was stirred at room temperature for 12 h. The mixture was then filtered through celite, the filtrate was dried over MgSO₄, and the solvent was evaporated in vacuum. Further purification was performed by column chromatography using *n*-hexane/EtOAc (5:1) as mobile phase to obtain the title compound as yellow solid (0.53 g, 38%). ^{1}H NMR (250 MHz, DMSO-*d₆*) δ = 8.50 (d, *J* = 2.2 Hz, 1H), 8.02 (dd, *J* = 9.1, 2.3 Hz, 1H), 7.59 (d, *J* = 9.1 Hz, 1H), 7.53 – 7.45 (m, 2H), 7.37 (s, 1H), 7.28 (d, *J* = 8.3 Hz, 1H), 4.12 (s, 2H), 3.92 (s, 3H), 3.83 (s, 3H), 3.81 (s, 3H). MS (ESI+): *m/z* 377.05 [M+Na]⁺.

Methyl 4-((5-amino-1-methyl-1*H*-indol-3-yl)methyl)-3-methoxybenzoate (**16**): Methyl 3-methoxy-4-((1-methyl-5-nitro-1*H*-indol-3-yl)methyl)benzoate (**15**, 0.17 g, 0.50 mmol, 1.0 eq) was dissolved in 10 mL EtOH and Pd(C) (53 mg, 0.05 mmol, 0.1 eq) was added. The suspension was stirred at room temperature under H₂ atmosphere for 12 h. The mixture was then filtered through celite, the filtrate was dried over MgSO₄, and the solvent was evaporated in vacuum to obtain the title compound as pale purple solid (0.15 g, 94%). ^{1}H NMR (250 MHz, DMSO-*d₆*) δ = 7.53 – 7.41 (m, 2H), 7.16 – 7.01 (m, 2H), 6.88 (s, 1H), 6.59 – 6.48 (m, 2H), 4.44 (br s, 2H), 3.95 – 3.87 (m, 5H), 3.83 (s, 3H), 3.62 (s, 3H). MS (ESI+): *m/z* 325.19 [M+H]⁺.

Methyl 4-((5-(3-cyclohexylureido)-1-methyl-1*H*-indol-3-yl)methyl)-3-methoxybenzoate (**21**): Methyl 4-((5-amino-1-methyl-1*H*-indol-3-yl)methyl)-3-methoxybenzoate (**16**, 487

mg, 1.50 mmol, 1.00 eq) was dissolved in THF (abs., 22 mL) and DBU (abs., 0.75 mL) was added. Cyclohexylisocyanate (**19**, 281 mg, 2.25 mmol, 1.50 eq) was added dropwise and the mixture was stirred at 40°C for 12 h. 30 mL 1% aqueous hydrochloric acid were added and the mixture was stirred for another 5 minutes. After addition of 15 mL EtOAc phases were separated and the aqueous layer was extracted with EtOAc (2x30 mL). The combined organic layers were dried over Na_2SO_4 and the solvents were evaporated under reduced pressure. The crude product was purified by column chromatography using EtOAc/hexane (1:4) as mobile phase to yield the title compound as colorless solid (330 mg, 49%). ^{1}H NMR (400 MHz, DMSO-d_6) δ = 8.03 (s, 1H), 7.50 (d, J = 1.3 Hz, 2H), 7.46 (dd, J = 7.8, 1.5 Hz, 1H), 7.25 (d, J = 8.7 Hz, 1H), 7.14 (d, J = 7.8 Hz, 1H), 7.05 (dd, J = 8.7, 1.9 Hz, 1H), 7.02 (s, 1H), 5.86 (d, J = 7.8 Hz, 1H), 3.96 (s, 2H), 3.93 (s, 3H), 3.84 (s, 3H), 3.69 (s, 3H), 3.53 – 3.39 (m, 1H), 1.85 – 1.76 (m, 2H), 1.71 – 1.62 (m, 2H), 1.59 – 1.50 (m, 1H), 1.38 – 1.07 (m, 5H). MS (ESI+): m/z 450.1 [M+H]$^+$.

4-((5-(3-Cyclohexylureido)-1-methyl-1H-indol-3-yl)methyl)-3-methoxybenzoic acid (**24**): Methyl 4-((5-(3-cyclohexylureido)-1-methyl-1H-indol-3-yl)methyl)-3-methoxybenzoate (**21**, 310 mg, 0.69 mmol, 1.00 eq) was dissolved in methanol (6 mL), water (12 mL) and lithium hydroxide (198 mg, 8.28 mmol, 12.0 eq) were added and the mixture was stirred at room temperature for 16 h. After acidification with 20 mL 10% aqueous hydrochloric acid, the mixture was extracted with EtOAc (3x25 mL). The combined organic layers were dried over Na_2SO_4 and the solvents were evaporated under reduced pressure. The crude product was purified by column chromatography using EtOAc/hexane/acetic acid (19:79:2) as mobile phase to yield the title compound as colorless solid (265 mg, 88%). ^{1}H NMR (500 MHz, DMSO-d_6) δ = 8.03 (s, 1H), 7.48 (d, J = 1.6 Hz, 2H), 7.42 (dd, J = 7.8, 1.5 Hz, 1H), 7.23 (d, J = 8.7 Hz, 1H), 7.09 (d, J = 7.8 Hz, 1H), 7.04 (dd, J = 8.7, 2.0 Hz, 1H), 7.00 (s, 1H), 5.86 (d, J = 7.9 Hz, 1H), 3.94 (s, 2H), 3.90 (s, 3H), 3.68 (s, 3H), 3.45 – 3.41 (m, 1H), 1.82 – 1.75 (m, 2H), 1.65 (dd, J = 9.1, 4.1 Hz, 2H), 1.53 (dd, J = 8.5, 4.1 Hz, 1H), 1.34 – 1.23 (m, 2H), 1.21 – 1.08 (m, 3H). MS (ESI-): m/z 434.29 [M-H]$^-$.

ASSOCIATED CONTENT

Supporting Information contains supporting figures, synthetic procedures, analytical characterization and methods for in vitro/in vivo characterization.
Molecular Formula Strings.
This material is available free of charge via the Internet at http://pubs.acs.org.

AUTHOR INFORMATION

Corresponding Author

* Daniel Merk. Phone +49 69 798 29327. E-mail: merk@pharmchem.uni-frankfurt.de

Author Contributions

# S.S. and C.F. contributed equally to first authorship. ## E.P. and D.M. contributed equally to senior authorship. All authors have given approval to the final version of the manuscript.

Notes

The authors declare no competing financial interest.
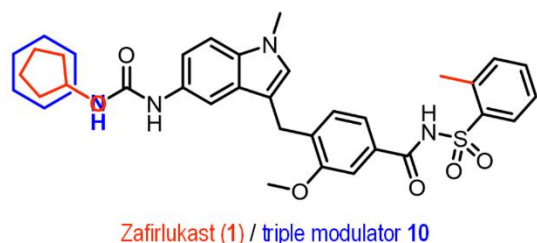
ACKNOWLEDGMENT

ABBREVIATIONS

AIBN, 2,2'-azobis(2-methylpropionitrile); CD36, cluster of differentiation 36; CAR, constitutive androstane receptor; CIU, N-cyclohexyl-N'-(4-iodophenyl)urea; CysLT$_1$R, cysteinyl leukotriene receptor 1; DCC, dicyclohexylcarbodiimide; DHET, dihydroxyeicosatrienoic acid; DIPEA, N,N-diisopropylethylamine; DMAP, 4-(dimethylamino)pyridine; DMS, dimethyl sulfate; DNA, deoxyribonucleic acid; EC$_{50}$, half maximal effective concentration; EET, epoxyeicosatrienoic acid; EtOAc, ethyl acetate; HEK293T, human embryonic kidney cells 293T; HepG2, human hepatoma cells; IC$_{50}$, half maximal inhibitory concentration; LBD, ligand binding domain; NBS, N-bromosuccinimide; PHOME, 3-phenylcyano-(6-methoxy-2-naphthalenyl)-2-oxiraneacetic acid methyl ester; PPAR, peroxisome proliferator-activated receptor; PXR, pregnane x receptor; THF, tetrahydrofuran; sEH, soluble epoxide hydrolase; SEM, standard error of the mean.

REFERENCES

(1)   Hanke, T.; Merk, D.; Steinhilber, D.; Geisslinger, G.; Schubert-Zsilavecz, M. Small Molecules with Anti-Inflammatory Properties in Clinical Development. *Pharmacol. Ther.* **2016**, *157*, 163–187.

(2)   Lötsch, J.; Geisslinger, G. Low-Dose Drug Combinations along Molecular Pathways Could Maximize Therapeutic Effectiveness While Minimizing Collateral Adverse Effects. *Drug Discov. Today* **2011**, *16* (23–24), 1001–1006.

(3)   Bäck, M.; Dahlén, S.-E.; Drazen, J. M.; Evans, J. F.; Serhan, C. N.; Shimizu, T.; Yokomizo, T.; Rovati, G. E. International Union of Basic and Clinical Pharmacology. LXXXIV: Leukotriene Receptor Nomenclature, Distribution, and Pathophysiological Functions. *Pharmacol. Rev.* **2011**, *63* (3), 539–584.

(4)   Bäck, M.; Powell, W. S.; Dahlén, S.-E.; Drazen, J. M.; Evans, J. F.; Serhan, C. N.; Shimizu, T.; Yokomizo, T.; Rovati, G. E. Update on Leukotriene, Lipoxin and Oxoeicosanoid Receptors: IUPHAR Review 7. *Br. J. Pharmacol.* **2014**, *171* (15), 3551–3574.

(5)   Sarau, H. M.; Ames, R. S.; Chambers, J.; Ellis, C.; Elshourbagy, N.; Foley, J. J.; Schmidt, D. B.; Muccitelli, R. M.; Jenkins, O.; Murdock, P. R.; Herrity, N. C.; Halsey, W.; Sathe, G.; Muir, A. I.; Nuthulaganti, P.; Dytko, G. M.; Buckley, P. T.; Wilson, S.; Bergsma, D. J.; Hay, D. W. P. Identification, Molecular Cloning, Expression, and Characterization of a Cysteinyl Leukotriene Receptor. *Mol. Pharmacol.* **1999**, *56* (3), 657–663.

(6)   Michalik, L.; Auwerx, J.; Berger, J. P.; Chatterjee, V. K.; Glass, C. K.; Gonzalez, F. J.; Grimaldi, P. A.; Kadowaki, T.; Lazar, M. A.; O'Rahilly, S.; Palmer, C. N. A.; Plutzky, J.; Reddy, J. K.; Spiegelman, B. M.; Staels, B.; Wahli, W. International Union of Pharmacology. LXI. Peroxisome Proliferator-Activated Receptors. *Pharmacol. Rev.* **2006**, *58* (4), 726–741.

(7)   Shen, H. C.; Hammock, B. D. Discovery of Inhibitors of Soluble Epoxide Hydrolase: A Target with Multiple Potential Therapeutic Indications. *J. Med. Chem.* **2012**, *55* (5), 1789–1808.

(8)   Zimmer, B.; Angioni, C.; Osthues, T.; Toewe, A.; Thomas, D.; Pierre, S. C.; Geisslinger, G.; Scholich, K.; Sisignano, M. The Oxidized Linoleic Acid Metabolite 12,13-DiHOME Mediates Thermal Hyperalgesia during Inflammatory Pain. *Biochim. Biophys. Acta - Mol. Cell Biol. Lipids* **2018**, *1863* (7), 669–678.

(9)   Cuzzocrea, S.; Pisano, B.; Dugo, L.; Ianaro, A.; Maffia, P.; Patel, N. S. A.; Di Paola, R.; Ialenti, A.; Genovese, T.; Chatterjee, P. K.; Di Rosa, M.; Caputi, A. P.; Thiemermann, C. Rosiglitazone, a Ligand of the Peroxisome Proliferator-Activated Receptor-Gamma, Reduces Acute Inflammation. *Eur. J. Pharmacol.* **2004**, *483* (1), 79–93.

(10) Proschak, E.; Heitel, P.; Kalinowsky, L.; Merk, D. Opportunities

and Challenges for Fatty Acid Mimetics in Drug Discovery. *J. Med. Chem.* **2017**, *60* (13), 5235–5266.

(11) Öster, L.; Tapani, S.; Xue, Y.; Käck, H. Successful Generation of Structural Information for Fragment-Based Drug Discovery. *Drug Discov. Today* **2015**, *20* (9), 1104–1111.

(12) Goverdhan, G.; Reddy, A. R.; Himabindu, V.; Reddy, G. M. Concise and Alternative Synthesis of Zafirlukast, an Anti-Asthma Drug. *Synth. Commun.* **2013**, *43* (4), 498–504.

(13) Schmidt, J.; Rotter, M.; Weiser, T.; Wittmann, S.; Weizel, L.; Kaiser, A.; Heering, J.; Goebel, T.; Angioni, C.; Wurglics, M.; Paulke, A.; Geisslinger, G.; Kahnt, A.; Steinhilber, D.; Proschak, E.; Merk, D. A Dual Modulator of Farnesoid X Receptor and Soluble Epoxide Hydrolase to Counter Nonalcoholic Steatohepatitis. *J. Med. Chem.* **2017**, *60* (18), 7703–7724.

(14) Moser, D.; Achenbach, J.; Klingler, F.-M.; Estel la, B.; Hahn, S.; Proschak, E. Evaluation of Structure-Derived Pharmacophore of Soluble Epoxide Hydrolase Inhibitors by Virtual Screening. *Bioorg. Med. Chem. Lett.* **2012**, *22* (21), 6762–6765.

(15) Capra, V.; Carnini, C.; Accomazzo, M. R.; Di Gennaro, A.; Fiumicelli, M.; Borroni, E.; Brivio, I.; Buccellati, C.; Mangano, P.; Carnevali, S.; Rovati, G.; Sala, A. Autocrine Activity of Cysteinyl Leukotrienes in Human Vascular Endothelial Cells: Signaling through the CysLT2 Receptor. *Prostaglandins Other Lipid Mediat.* **2015**, *120*, 115–125.

(16) Kim, K. R.; Lee, J. H.; Kim, S. J.; Rhee, S. D.; Jung, W. H.; Yang, S.-D.; Kim, S. S.; Ahn, J. H.; Cheon, H. G. KR-62980: A Novel Peroxisome Proliferator-Activated Receptor γ Agonist with Weak Adipogenic Effects. *Biochem. Pharmacol.* **2006**, *72* (4), 446–454.

(17) Kim, M.-K.; Chae, Y. N.; Choi, S.; Moon, H. S.; Son, M.-H.; Bae, M.-H.; Choi, H.; Hur, Y.; Kim, E.; Park, Y. H.; Park, C. S.; Kim, J. G.; Lim, J. I.; Shin, C. Y. PAM-1616, a Selective Peroxisome Proliferator-Activated Receptor γ Modulator with Preserved Anti-Diabetic Efficacy and Reduced Adverse Effects. *Eur. J. Pharmacol.* **2011**, *650* (2–3), 673–681.

(18) Gellrich, L.; Merk, D. Therapeutic Potential of Peroxisome Proliferator-Activated Receptor Modulation in Non-Alcoholic Fatty Liver Disease and Non-Alcoholic Steatohepatitis. *Nucl. Recept. Res.* **2017**, *4*, 101310.

(19) Lim, Y.-P.; Huang, J. Interplay of Pregnane X Receptor with Other Nuclear Receptors on Gene Regulation. *Drug Metab. Pharmacokinet.* **2008**, *23* (1), 14–21.

(20) Prakash, C.; Zuniga, B.; Seog Song, C.; Jiang, S.; Cropper, J.; Park, S.; Chatterjee, B. Nuclear Receptors in Drug Metabolism, Drug Response and Drug Interactions. *Nucl. Recept. Res.* **2015**, *2*, 101178.

(21) Meller, S. T.; Gebhart, G. F. Intraplantar Zymosan as a Reliable, Quantifiable Model of Thermal and Mechanical Hyperalgesia in the Rat. *Eur. J. Pain* **1997**, *1* (1), 43–52.

(22) Park, S. J.; Lee, K. S.; Kim, S. R.; Min, K. H.; Choe, Y. H.; Moon, H.; Chae, H. J.; Yoo, W. H.; Lee, Y. C. Peroxisome Proliferator-Activated Receptor   Agonist Down-Regulates IL-17 Expression in a Murine Model of Allergic Airway Inflammation. *J. Immunol.* **2009**, *183* (5), 3259–3267.

(23) Smith, S. G.; Hill, M.; Oliveria, J.-P.; Watson, B. M.; Baatjes, A. J.; Dua, B.; Howie, K.; Campbell, H.; Watson, R. M.; Sehmi, R.; Gauvreau, G. M. Evaluation of Peroxisome Proliferator-Activated Receptor Agonists on Interleukin-5-Induced Eosinophil Differentiation. *Immunology* **2014**, *142* (3), 484–491.

(24) Bourke, J. E.; Bai, Y.; Donovan, C.; Esposito, J. G.; Tan, X.; Sanderson, M. J. Novel Small Airway Bronchodilator Responses to Rosiglitazone in Mouse Lung Slices. *Am. J. Respir. Cell Mol. Biol.* **2014**, *50* (4), 748–756.

(25) Won, H. Y.; Min, H. J.; Ahn, J. H.; Yoo, S.-E.; Bae, M. A.; Hong, J.-H.; Hwang, E. S. Anti-Allergic Function and Regulatory Mechanisms of KR62980 in Allergen-Induced Airway Inflammation. *Biochem. Pharmacol.* **2010**, *79* (6), 888–896.

(26) Oh, S.-H.; Park, S.-M.; Lee, Y. H.; Cha, J. Y.; Lee, J.-Y.; Shin, E. K.; Park, J.-S.; Park, B.-L.; Shin, H. D.; Park, C.-S. Association of Peroxisome Proliferator-Activated Receptor-Gamma Gene Polymorphisms with the Development of Asthma. *Respir. Med.* **2009**, *103* (7), 1020–1024.

(27) Yang, J.; Bratt, J.; Franzi, L.; Liu, J.-Y.; Zhang, G.; Zeki, A. A.; Vogel, C. F. A.; Williams, K.; Dong, H.; Lin, Y.; Hwang, S. H.; Kenyon, N. J.; Hammock, B. D. Soluble Epoxide Hydrolase Inhibitor Attenuates Inflammation and Airway Hyperresponsiveness in Mice. *Am. J. Respir. Cell Mol. Biol.* **2015**, *52* (1), 46–55.

(28) Lakshmi, S. P.; Reddy, A. T.; Zhang, Y.; Sciurba, F. C.; Mallampalli, R. K.; Duncan, S. R.; Reddy, R. C. Down-Regulated Peroxisome Proliferator-Activated Receptor γ (PPARγ) in Lung Epithelial Cells Promotes a PPARγ Agonist-Reversible Proinflammatory Phenotype in Chronic Obstructive Pulmonary Disease (COPD). *J. Biol. Chem.* **2014**, *289* (10), 6383–6393.

(29) Rinne, S.; Feemster, L.; Collins, B.; Liu, C.-F.; Bryson, C.; O'Riordan, T.; Au, D. Thiazolidinediones Are Associated with a Reduced Risk of COPD Exacerbations. *Int. J. Chron. Obstruct. Pulmon. Dis.* **2015**, *10*, 1591.

(30) Cazzola, M.; Boveri, B.; Carlucci, P.; Santus, P.; DiMarco, F.; Centanni, S.; Allegra, L. Lung Function Improvement in Smokers Suffering from COPD with Zafirlukast, a CysLT1-Receptor Antagonist. *Pulm. Pharmacol. Ther.* **2000**, *13* (6), 301–305.

(31) Zhou, Y.; Sun, G. Y.; Liu, T.; Duan, J. X.; Zhou, H. F.; Lee, K. S.; Hammock, B. D.; Fang, X.; Jiang, J. X.; Guan, C. X. Soluble Epoxide Hydrolase Inhibitor 1-Trifluoromethoxyphenyl-3-(1-Propionylpiperidin-4-Yl) Urea Attenuates Bleomycin-Induced Pulmonary Fibrosis in Mice. *Cell Tissue Res.* **2016**, *363* (2), 399–409.

(32) Wang, L.; Yang, J.; Guo, L.; Uyeminami, D.; Dong, H.; Hammock, B. D.; Pinkerton, K. E. Use of a Soluble Epoxide Hydrolase Inhibitor in Smoke-Induced Chronic Obstructive Pulmonary Disease. *Am. J. Respir. Cell Mol. Biol.* **2012**, *46* (5), 614–622.

(33) Wermuth, C. G. Selective Optimization of Side Activities: The SOSA Approach. *Drug Discov. Today* **2006**, *11* (3–4), 160–164.

Zafirlukast (1) / triple modulator 10

pEC$_{50}$(PPARγ) = 5.6 / 6.5, pIC$_{50}$(sEH) = 5.7 / 7.4, pA$_2$(CysLT$_1$R) = 11.4 / 8.7

zymosan induced paw edema

Table of Contents graphic

1
2
3
4
5
6
7
8
9
10
11
12
13
14
15
16
17
18
19
20
21
22
23
24
25
26
27
28
29
30
31
32
33
34
35
36
37
38
39
40
41
42
43
44
45
46
47
48
49
50
51
52
53
54
55
56
57
58
59
60
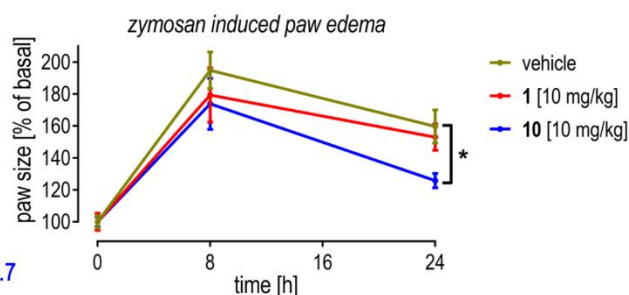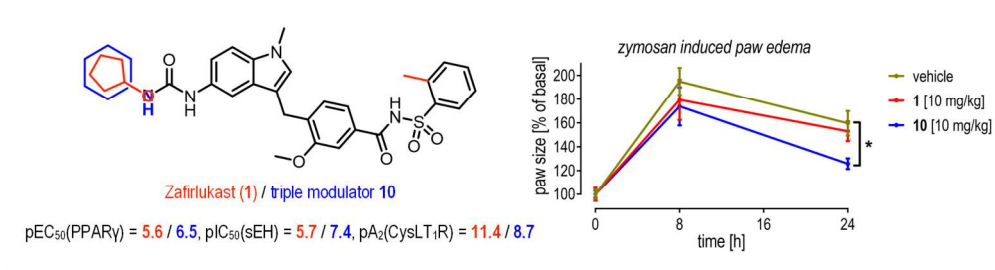

Table of Contents graphic

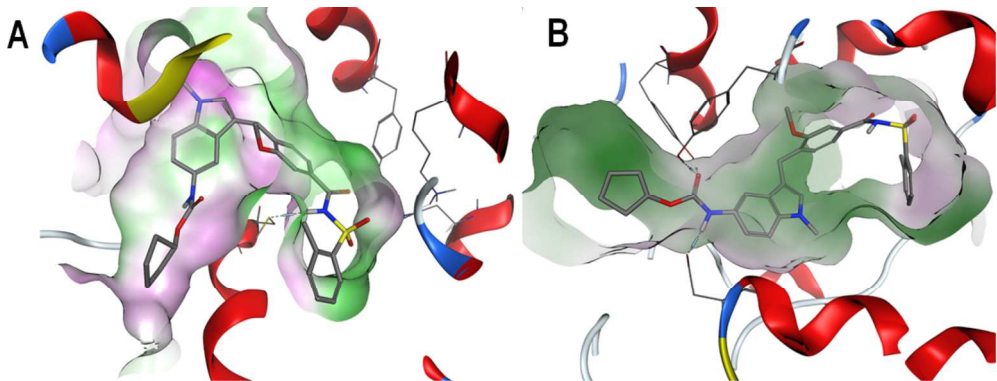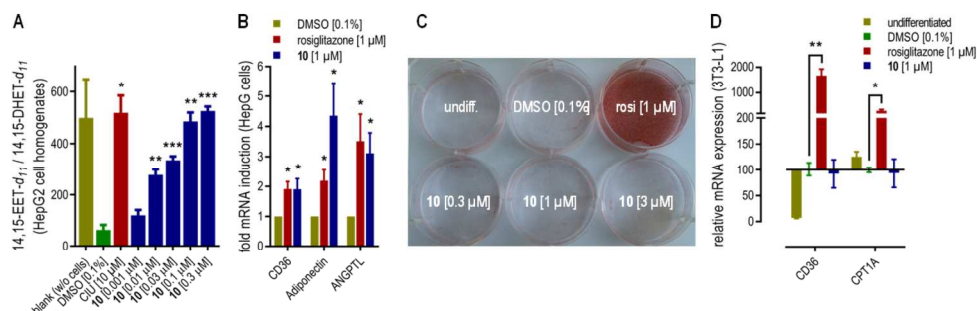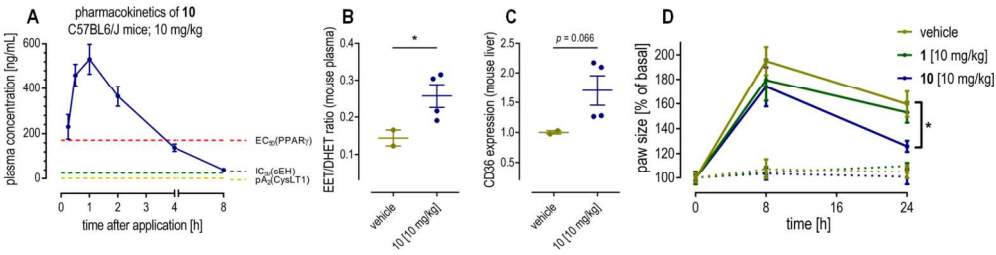209x55mm (300 x 300 DPI)

Figure 1

523x196mm (96 x 96 DPI)

Figure 2

870x285mm (96 x 96 DPI)

Figure 3

762x193mm (96 x 96 DPI)